

Superconductivity in the Uniform Electron Gas: Irrelevance of Kohn-Luttinger Mechanism

Xiansheng Cai and Tao Wang

Department of Physics, University of Massachusetts, Amherst, MA 01003, USA

Nikolay V. Prokof'ev*

*Department of Physics, University of Massachusetts, Amherst, MA 01003, USA and
National Research Center "Kurchatov Institute," 123182 Moscow, Russia*

Boris V. Svistunov†

*Department of Physics, University of Massachusetts, Amherst, MA 01003, USA
National Research Center "Kurchatov Institute," 123182 Moscow, Russia and
Wilczek Quantum Center, School of Physics and Astronomy,
Shanghai Jiao Tong University, Shanghai 200240, China*

Kun Chen‡

*Center for Computational Quantum Physics, Flatiron Institute, 162 5th Avenue, New York, New York 10010
(Dated: February 10, 2022)*

We study the Cooper instability in jellium model in the controlled regime of small to intermediate values of the Coulomb parameter $r_s \leq 2$. We confirm that superconductivity naturally emerges from purely repulsive interactions described by the Kukkonen-Overhauser vertex function. By employing the implicit renormalization approach we reveal that even in the small- r_s limit, the dominant mechanism behind Cooper instability is based on dynamic screening of the Coulomb interaction—accurately captured by the random phase approximation, whereas the Kohn-Luttinger contribution is negligibly small and, thus, not relevant.

Introduction.—Conventional BCS theory predicts Cooper instability at low temperature in a Fermi liquid with weak short range attractive coupling between the low-energy electrons, typically originating from the electron-phonon interaction (EPI). With the discovery of unconventional superconducting systems, such as d -wave cuprate superconductors [1–4], s^{+-} Fe-based superconductors [5–8], multi-layer graphene systems [9–12], etc., alternative theories of Cooper instability have been drawing great research interest. In the last decades, a number of different mechanisms were proposed for the pairing instability in systems where the EPI alone was not sufficient to explain the data [13–17]. Some of them are based on purely repulsive bare electron-electron interactions [13–15]. In this work, we revisit superconducting properties of the uniform electron gas (jellium model) where pairing instability takes place in a Coulomb system with purely repulsive interparticle interactions and Fermi energy is the only relevant energy scale (all other energy scales are emergent). Our prime focus is the quantitative study of two canonical scenarios emerging from renormalized interactions: the Kohn-Luttinger (KL) mechanism based on the $2k_F$ singularity (where k_F is the Fermi momentum) and the dynamic screening mechanism.

In 1965, Kohn and Luttinger argued that for any weak short-range repulsive interaction, the two-particle effective interaction induced by many-body effects always becomes attractive at large enough orbital momenta $\ell \gg 1$, and could lead to Cooper instability [13]. They used

the same analysis to estimate an effective Cooper channel coupling for the static screened Coulomb interaction, which can be considered as a weak short-range one in the high-density limit $r_s \rightarrow 0$. The KL mechanism has motivated a series of theoretical attempts to explain unconventional superconducting systems using repulsive interactions [18–20], and is widely believed to be the dominant mechanism leading to superconductivity in jellium at small r_s . However, a thorough investigation of the dominant mechanism leading to superconductivity in this system is still missing: (i) Analytical KL approach based on the static screened Coulomb interaction is an uncontrolled approximation; (ii) We are not aware of any challenging numerical study of the KL mechanism because it only emerges at large ℓ and leads to extremely small values of T_c ; (iii) Whenever Cooper instability is observed in the simulation, one needs to differentiate between different scenarios behind it by revealing and evaluating their contributions separately. Therefore, whether the KL mechanism ever becomes dominant in the uniform electron gas in the high-density limit $r_s \rightarrow 0$ is still an unsolved fundamental question.

It has been known for decades that dynamic screening of Coulomb interaction could also induce the pairing instability in the uniform electron gas. The early work by Tolmachev [21] demonstrated that even if the Cooper channel coupling is repulsive at all frequencies, after its high-frequency part is renormalized to a smaller value the net result might be an attractive low-frequency effective

potential. Later, Takada and others calculated the critical temperatures T_c of the uniform electron gas numerically with using various forms of dynamically screened Coulomb interaction [14, 15, 22, 23]. Subsequent studies also reported that dynamic screening plays an important role in the superconductivity of metallic hydrogen and alkali metals [24, 25] as well as in the dilute electron gas [16]. The superconducting phase diagram produced by Takada [23] showed that the uniform electron gas enters a normal phase at $r_s < 2.0$, in contradiction with the KL prediction. Almost certainly, the values of T_c at large ℓ were too small to be resolved and, therefore, were ignored for practical purposes. Because of this limitation, KL and dynamic screening mechanisms have never been quantitatively compared to each other, despite their co-existence in the uniform electron gas.

To determine which mechanism is dominant in the uniform electron gas and under what conditions, we study the Cooper instability in the controlled regime of small to intermediate values of $r_s \leq 2$. The particle-particle irreducible four-point vertex is approximated with the Kukkonen-Overhauser (KO) interaction [26], which becomes exact in the high-density limit $r_s \rightarrow 0$. We compare contributions from both mechanisms in two different ways. The first protocol follows the standard approach when T_c is calculated by solving for the largest eigenvalue, $\lambda(T)$, of the gap equation and determining when $\lambda(T = T_c) = 1$. The $\lambda(T)$ curve can be computed down to $T/E_F = 10^{-6}$ (below we use Fermi energy E_F as the unit of energy). We then remove the $q = 2k_F$ singularity in the polarization function, on which the KL mechanism is based, from the effective interaction, and measure the relative change of the eigenvalue, $\eta(T) = \delta\lambda/\lambda$. Finally, we extrapolate results to T_c and estimate $\eta(T_c)$, which represents the relative contribution of the KL mechanism. This perturbative treatment is justified if $\eta(T)$ is small, which turns out to be always the case. The second protocol is based on the recently proposed implicit renormalization (IR) approach [27]. By implicitly integrating out the high-frequency/energy degrees of freedom the IR approach solves a new eigenvalue problem for which the largest eigenvalue, $\bar{\lambda}(T)$, is also equal to unity at $T = T_c$. The crucial advantage of looking at $\bar{\lambda}(T)$ instead of $\lambda(T)$ is that its temperature dependence is a linear function of $\ln(T)$ for a properly chosen energy separation scale, and, thus, can be accurately extrapolated to T_c from $T \gg T_c$. Computational costs are further dramatically reduced by employing the discrete Lehmann representation (DLR) [28]. This combination of methods is what allows us to determine the superconducting channel ℓ_c with the highest value of T_c at $r_s = 0.33, 0.5, 1, 2$; otherwise, the problem cannot be solved by the standard approach. By computing the critical values of orbital channels, $\ell_{KL}(r_s)$, when the KL mechanism first induces an attractive Cooper channel coupling, and comparing the asymptotic behavior of ℓ_c and ℓ_{KL} at small r_s we

determine what mechanism is dominating in the high-density limit.

Within the first protocol we find that the contribution of the KL mechanism remains extremely small, and therefore irrelevant, for any value of r_s when the transition temperatures exceed 10^{-10^6} . The second protocol reveals that the Cooper instability in the uniform electron gas takes place at all values of r_s tested. More importantly, the dominant channel ℓ_c increases much slower than the critical channel of the KL mechanism, ℓ_{KL} , as r_s decreases, indicating that in the high-density limit superconductivity is induced by the dynamic screening effects—accurately captured by the random phase approximation—well before the KL mechanism could have any impact.

Model.—Jellium model is defined by the Hamiltonian

$$H = \sum_{\mathbf{k}\sigma} \epsilon_{\mathbf{k}} a_{\mathbf{k}\sigma}^\dagger a_{\mathbf{k}\sigma} + \frac{1}{2} \sum_{\mathbf{q}, \mathbf{k}, \mathbf{k}', \sigma, \sigma'}^{q \neq 0} V_{\mathbf{q}} a_{\mathbf{k}+\mathbf{q}\sigma}^\dagger a_{\mathbf{k}'-\mathbf{q}\sigma'}^\dagger a_{\mathbf{k}'\sigma'} a_{\mathbf{k}\sigma}, \quad (1)$$

with $a_{\mathbf{k}\sigma}^\dagger$ the creation operator of an electron with momentum \mathbf{k} and spin $\sigma = \uparrow, \downarrow$, dispersion $\epsilon_{\mathbf{k}} = \frac{k^2}{2m_e} - \mu$, and Coulomb potential $V_{\mathbf{q}} = \frac{e^2}{\epsilon_0 q^2}$. The dimensionless coupling parameter (the Wigner-Seitz radius) is given by $r_s = \frac{1}{a_0} \left(\frac{3}{4\pi n} \right)^{\frac{1}{3}}$, where n is the number density, and a_0 is the Bohr radius.

To obtain the critical temperature and gap function one needs to solve the eigenvalue equation in the Cooper channel

$$\lambda(T) \Delta_{\omega_n, \mathbf{k}} = -T \sum_m \int \frac{d\mathbf{p}}{(2\pi)^d} \Gamma_{\omega_n, \mathbf{p}}^{\omega_n, \mathbf{k}} G_{\omega_m, \mathbf{p}} G_{-\omega_m, -\mathbf{p}} \Delta_{\omega_m, \mathbf{p}}. \quad (2)$$

Here Γ is the particle-particle irreducible four-point vertex, G is the single particle Green's function, and Δ is the gap function with an eigenvalue λ . The key approximation used in this work is the Kukkonen-Overhauser ansatz [26] for Γ (see also the Supplemental Material):

$$V_{\vec{\sigma}\vec{\sigma}'}^{KO}(\omega, q) = V_q + V_+(q)^2 Q_+(\omega, q) + V_-(q)^2 Q_-(\omega, q) \vec{\sigma} \cdot \vec{\sigma}', \quad (3)$$

with

$$Q_{\pm}(\omega, q) = -\frac{\Pi_0(\omega, q)}{1 + V_{\pm}(\omega, q) \Pi_0(\omega, q)}, \quad (4)$$

$$V_+ = (1 - G_+)V, \quad V_- = -G_-V. \quad (5)$$

It is defined in terms of the polarization function $\Pi_0 = G_0 G_0$ based on the convolution of bare Green's functions, G_0 , and local field factors $G_{\pm}(q)$. When $G_{\pm}(q)$ are set to zero, the KO interaction reduces to the random phase approximation (RPA). The local field factors encode the many-body exchange and correlation effects beyond RPA. For direct comparison with previous work

by Takada we adopt the same ansatz for $G_{\pm}(q)$ [22, 23], and take the functional form of Π_0 to be that at $T = 0$:

$$\Pi_0(q, \omega) \simeq \frac{mk_F}{2\pi^2} P\left(\frac{q}{2k_F}, \frac{m\omega}{qk_F}\right), \quad (6)$$

$$P(z, u) = 1 + \frac{1 - z^2 + u^2}{4z} \ln \frac{(1+z)^2 + u^2}{(1-z)^2 + u^2} - u \tan^{-1} \frac{2u}{u^2 + z^2 - z}. \quad (7)$$

This is justified by the smallness of the critical temperature. The gap equation is decomposed into different orbital channels, ℓ , which are solved independently. The critical temperature T_c in each channel corresponds to the point where the largest eigenvalue $\lambda(T)$ equals unity.

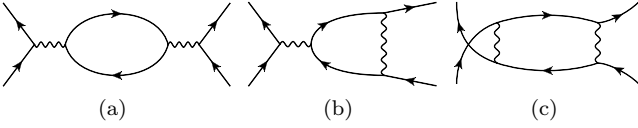


FIG. 1: Second-order diagrams that contribute to the particle-particle irreducible four-point vertex Γ in the KL analysis. Only the first bubble diagram is resummed within the RPA approach, while all the three diagrams are resummed in the KO formulation. In the small- r_s limit, the contributions of the diagrams (b) and (c) might prove appreciable only if Kohn-Luttinger mechanism is the leading channel of Cooper instability; otherwise, all the leading contributions are accurately captured by RPA.

Kohn-Luttinger mechanism in the jellium model.—Cooper instability in the KL theory is induced by the logarithmic singularity in the static effective interaction at $q = 2k_F$ [13]. Within the second-order perturbation theory, it arises from diagrams shown in Fig. 1. After projecting static Γ to the ℓ -th orbital channel,

$$W_\ell(k, p, \omega = 0) = \int_{-1}^1 P_\ell(\chi) \Gamma(k, p, \chi, \omega = 0) d\chi, \quad (8)$$

where $\chi = \cos\theta$, with θ the angle between momenta \mathbf{k} and \mathbf{p} , and $P_\ell(\chi)$ are Legendre polynomials, Kohn and Luttinger found that in the large- ℓ limit, $W_\ell(k_F, k_F, \omega = 0)$ decays asymptotically as $1/\ell^4$ and oscillates between odd and even values of ℓ . The attractive effective coupling at large enough odd ℓ could then give rise to Cooper instability. The same analysis was also applied to the static screened Coulomb interaction in the high-density limit $r_s \rightarrow 0$, when it becomes equivalent to the weak short-range potential.

The KL treatment silently ignored the dynamic nature of screening despite the fact that at any finite frequency

the Coulomb potential cannot be screened at small momentum $q \ll \omega/v_F$. Moreover, singular nature of the Coulomb potential at small momentum calls for proper resummation of diagrams shown in Fig. 1 beyond the second-order perturbation theory. Clearly, a more controlled analysis is necessary to quantitatively evaluate the relative importance KL and dynamic screening effects in the jellium model.

Resummation of diagrams shown in Fig. 1 is achieved by the KO interaction, which thus provides an excellent framework for thorough investigation of competing mechanisms. In order to quantify the contribution of the $q = 2k_F$ singularity, we replace $\Pi_0(q, \omega)$ with the regularized ansatz

$$\Pi_\epsilon(q, \omega) = \frac{mk_F}{2\pi^2} P_\epsilon\left(\frac{q}{2k_F}, \frac{m\omega}{qk_F}\right), \quad (9)$$

$$P_\epsilon(z, u) = 1 + \frac{1 - z^2 + u^2}{4z} \ln \frac{(1+z)^2 + u^2}{(1-z)^2 + u^2 + \epsilon(z)} - u \tan^{-1} \frac{2u}{u^2 + z^2 - z}, \quad (10)$$

controlled by a parameter ϵ_0 in

$$\epsilon(z) = \epsilon_0 e^{-4(z-1)^2}. \quad (11)$$

The Gaussian limits all modification to the vicinity of the $2k_F$ singularity and ensures that changes in the eigenvalue λ can be attributed to the KL mechanism. To decide on the optimal value of ϵ_0 we computed $W_\ell(k_F, k_F, \omega = 0)$ (with the vertex function Γ replaced by the KO interaction) and settled on $\epsilon_0 = 0.001$ when oscillations in $W_\ell(k_F, k_F, \omega = 0)$ are almost completely removed, see Fig. 2. The next step is to study the effect of finite ϵ_0 on the gap equation eigenvalues λ_ℓ .

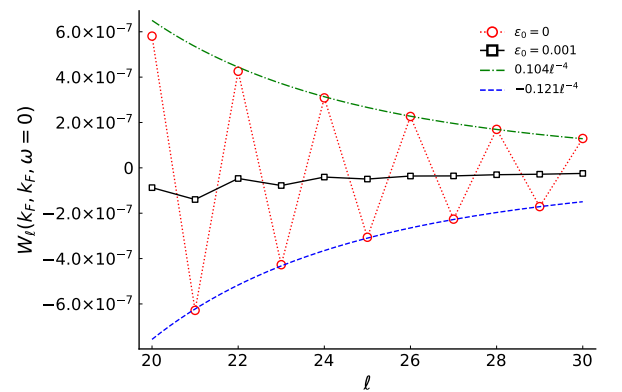


FIG. 2: The static KO vertex function on the Fermi surface $W_\ell(k_F, k_F, \omega = 0)$ at $r_s = 1.0$. Dotted red line with circles represents the original W_ℓ with clear KL oscillations decaying as $1/\ell^4$ according to the dotdash green and dashed blue fits. The solid black line with squares represents the regularized W_ℓ .

Implicit renormalization approach.—It is impossible to solve the gap equation directly when the critical temperature is extremely small because the number of required Matsubara frequency points is getting too large. Thus, reliable extrapolation from $T \gg T_c$ is essential for determining where $\lambda(T) = 1$. Such an extrapolation can hardly be done for frequency-dependent vertexes because $\lambda(T)$ turns out to be an unknown nonlinear function of $\ln T$. The implicit renormalization (IR) approach proposed in Ref. [27] offers a solution to this problem. The idea is to decompose the gap function into two complementary parts, $\Delta = \Delta^{(1)} + \Delta^{(2)}$, with $\Delta_n^{(1)} = 0$ for $|\omega_n| > \Omega_c$, and $\Delta_n^{(2)} = 0$ for $|\omega_n| < \Omega_c$, and solve an eigenvalue problem for the low-energy part $\Delta_n^{(1)}$ only. [The integration of high-energy degrees of freedom with the IR protocol is achieving the same goal as the pseudopotential theory]. The new eigenvalue $\bar{\lambda}(T)$ is expected to have a nearly perfect linear dependence on $\ln T$ for a properly chosen energy scale separation. The IR approach allows us to accurately determine T_c as low as $10^{-20} E_F$ by extrapolating $\bar{\lambda}(T)$ from the $10^{-5} < T/E_F < 10^{-3}$ interval. Once the Tolmachev-McMillan logarithm [15, 21, 29] is accounted for, the linear flow of $\bar{\lambda}(T)$ illustrated in Fig. 3 provides direct access to the Coulomb pseudopotential μ^* in a given orbital channel ℓ . Note that the difference between μ^* of the KO and RPA vertex functions is smaller than a few percent for odd ℓ at $r_s \leq 2.0$ and even ℓ for $r_s \leq 1.0$. This indicates that higher-order vertex correction for considered values of r_s is negligible.

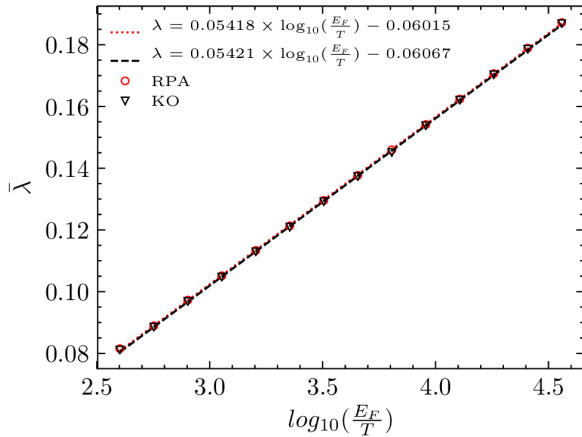


FIG. 3: Temperature dependence of the eigenvalues $\bar{\lambda}(T)$ for RPA (red circles) and KO (black triangles) vertex functions at $r_s = 2.0$ and $\ell = 3$. The linear fits of the RPA (red dotted line) and KO (black dashed line) data are almost identical.

Discrete Lehmann representation.—Even within the IR protocol, solving the gap equation at exponentially low temperature faces great challenges because the vertex function, the gap function, and the Green's function

are all multi-dimensional objects with nontrivial structure in momentum and frequency. The most important step to take is to optimize the Matsubara frequency grids to store just enough information for accurate interpolation of all functions. Fortunately, for a given ultraviolet cutoff ω_{\max} and numerical accuracy ϵ , the required grids are provided by the recently developed discrete Lehmann representation [28], or DLR. The number of grid points scales as $O(\ln(\omega_{\max}/T) \ln(\frac{1}{\epsilon}))$, and only 65 Matsubara frequencies are required to achieve accuracy $\epsilon = 10^{-10}$ at $\omega_{\max}/T = 10^5$. Fast implementation of all key operations including Fourier transforms interpolation and convolution are available within the DLR (see Supplemental Material for more details). By dramatically reducing memory and computational costs, the DLR grids allow us to simulate much lower temperatures and compute extremely small T_c . Specifically, we were able to determine the dominant superconducting orbital channel ℓ_c at $r_s \geq 0.33$.

Results.—In the upper panel of Fig. 4 we show the relative change of eigenvalues $\eta = \delta\lambda/\lambda$ at $T = 10^{-5} E_F$ when the KO function is regularized. At large ℓ we observe that η features the KL oscillation originating from the singularity in static vertex function $W_\ell(k_F, k_F, \omega = 0)$, superimposed on a slowly decaying background. The background is due to the vertex function modification in the finite vicinity of the $q = 2k_F$ point, and is not relevant for the KL mechanism. For this reason, the actual contribution of the $q = 2k_F$ singularity is characterized by the oscillation amplitude, which can be taken as the difference between the η_ℓ and $\eta_{\ell+1}$ values, see the lower panel in Fig. 4. Two immediate observations can be made: (i) the relative contribution of the KL mechanism is of the order of 10^{-7} ; (ii) the oscillation is less pronounced for smaller values of r_s . Both facts indicate that the KL mechanism is completely irrelevant for superconducting properties of jellium.

To ensure that these observations do not change with temperature, we performed simulations over a broad temperature range for $r_s = 0.5$, see Fig. 5. As the temperature goes down, we find that the KL contribution $\eta_{\ell+1} - \eta_\ell$ increases, but the rate is extremely small and decreases. Even if $\eta_{\ell+1} - \eta_\ell$ were to increase at a constant rate beyond $T/E_F = 10^{-6}$, it would still be smaller than a few percent at $T/E_F = 10^{-10}$, which is “zero” for all practical purposes.

Academically speaking (i.e., regardless of how small T_c is), the possibility of the KL superconductivity in the $r_s \rightarrow 0$ limit is not ruled out by results presented above because we cannot determine whether $\eta_{\ell+1} - \eta_\ell$ ultimately saturate to small values that decrease with r_s . However, recall that the KL mechanism can induce attractive coupling only at large enough $\ell \geq \ell_{KL}$. More precisely, $\ell_{KL}(r_s)$ is the first channel where $W_\ell(k_F, k_F, \omega = 0)$ becomes negative. It has to be compared with the IR solution for the dominant supercon-

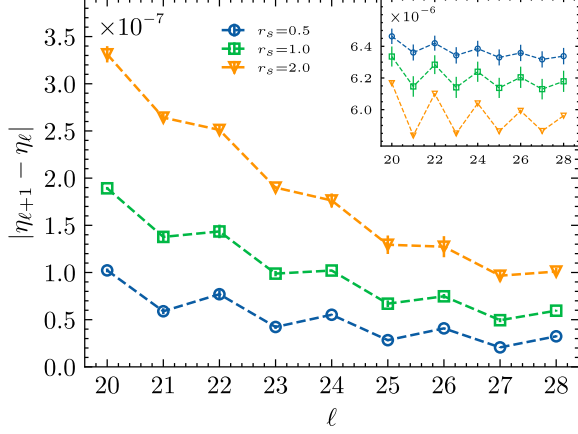


FIG. 4: Amplitudes of the relative eigenvalue oscillations, $|\eta_{\ell+1} - \eta_\ell|$, induced in the gap equation eigenvalues by regularization of the KO vertex at $T = 10^{-5} E_F$ and $r_s = 0.5$ (blue circles), $r_s = 1$ (green squares), and $r_s = 2$ (yellow triangles). Inset: relative eigenvalue changes η_ℓ . Note the scaling factors of 10^{-7} and 10^{-6} for the vertical axis in main figure and inset, respectively.

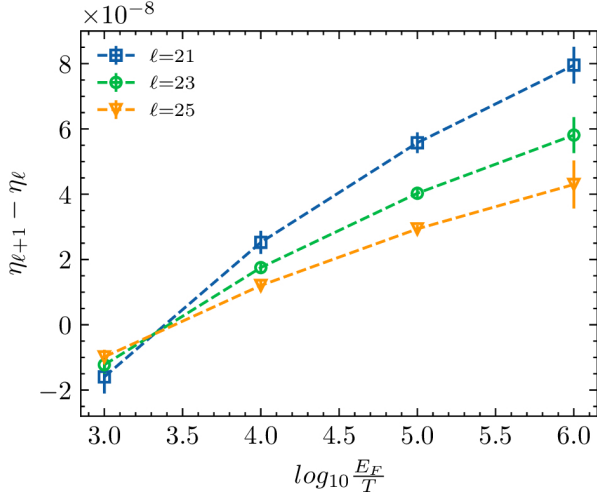


FIG. 5: The amplitude of the KL oscillation as a function of $\log_{10}(E_F/T)$ for $r_s = 0.5$, $\ell = 21$ (blue squares), $\ell = 23$ (green circles) and $\ell = 25$ (yellow triangles). When T/E_F is reduced by one order of magnitude, the oscillation amplitude increases by less than 3×10^{-8} for $\ell \geq 21$ at $T \sim 10^{-6} E_F$. The curve also shows signs of saturation as T/E_F decreases.

ducting channel, $\ell_c(r_s)$, when dealing with the dynamic KO vertex function (this can be done for $1/3 \leq r_s \leq 2$). The comparison presented in Fig. 6 clearly demonstrates that $\ell_{KL} > \ell_c$ for all r_s and the difference keeps growing when $r_s \rightarrow 0$. This means that superconductivity in the ℓ_c channel is induced by the dynamical screening well

before the KL mechanism becomes viable, including the $r_s \rightarrow 0$ limit.

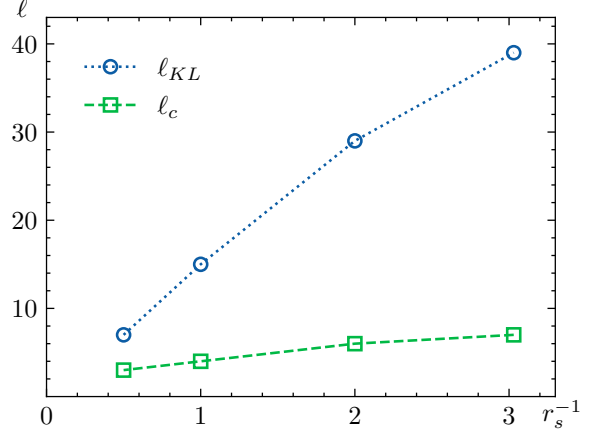


FIG. 6: Dominant superconducting channel ℓ_c (green squares connected by the dashed line) as a function of r_s along with the critical channel of the KL mechanism ℓ_{KL} (blue circles connected by the dotted line).

Discussion and conclusion.—In conclusion, we studied superconductivity in the jellium model for $r_s \leq 2$ by solving the gap equation based on the Kukkonen-Overhauser vertex function. We find that superconductivity naturally emerges from purely repulsive Coulomb potential once the dynamic screening effects are taken into account. We quantified the role of the Kohn-Luttinger mechanism, which is often assumed to be the prime reason behind Cooper instability in the high-density limit, and concluded that it is not relevant for two reasons: (i) For $r_s \leq 2$, the KL mechanism starts contributing to the Cooper instability only at orbital momenta ℓ_{KL} much larger than the dominant superconducting channel ℓ_c selected by the dynamic screening effect; (ii) For $\ell \geq \ell_{KL}$, the relative contribution of the KL mechanism is extremely small numerically, and can be safely ignored for all practical purposes. In particular, this implies that at $r_s \leq 1$, the physics of Cooper instability is controllably captured by the random phase approximation; thus posing a challenge of finding an accurate analytic proof of this fact in the $r_s \rightarrow 0$ limit.

Our work answers the fundamental question regarding the origin of Cooper instability in the homogeneous electron gas in the high-density limit, and revises the popular, yet incorrect, belief that the $q = 2k_F$ singularity is the dominant reason. Our approach offers a systematic way for studies of the Cooper instability in other correlated electronic systems.

The authors thank Carl Kukkonen for bringing the interplay between the Kukkonen-Overhauser interaction and the superconductivity to our attention. We also acknowledge Kristjan Haule for a stimulating discussion and for hosting a visit for two of the authors. Addition-

ally, K. Chen thanks Youjin Deng, Baozong Wang and Pengcheng Hou for helpful discussions. This work was supported by the the National Science Foundation under the grant DMR-2032077 and the Simons Collaboration on the Many Electron Problem. The Flatiron Institute is a division of the Simons Foundation.

* prokofev@physics.umass.edu

† svistunov@physics.umass.edu

‡ kunchen@flatironinstitute.org

- [1] J. G. Bednorz and K. A. Müller, *Z. Physik B - Condensed Matter* **64**, 189 (1986).
- [2] M. K. Wu, J. R. Ashburn, C. J. Torng, P. H. Hor, R. L. Meng, L. Gao, Z. J. Huang, Y. Q. Wang, and C. W. Chu, *Phys. Rev. Lett.* **58**, 908 (1987).
- [3] C. W. Chu, L. Gao, F. Chen, Z. J. Huang, R. L. Meng, and Y. Y. Xue, *Nature* **365**, 323 (1993).
- [4] C. C. Tsuei and J. R. Kirtley, *Rev. Mod. Phys.* **72**, 969 (2000).
- [5] Y. Kamihara, T. Watanabe, M. Hirano, and H. Hosono, *Journal of the American Chemical Society* **130**, 3296 (2008).
- [6] I. I. Mazin, D. J. Singh, M. D. Johannes, and M. H. Du, *Phys. Rev. Lett.* **101**, 057003 (2008).
- [7] F. Wang, H. Zhai, Y. Ran, A. Vishwanath, and D.-H. Lee, *Phys. Rev. Lett.* **102**, 047005 (2009).
- [8] Q. Si and E. Abrahams, *Phys. Rev. Lett.* **101**, 076401 (2008).
- [9] B. Uchoa and A. H. Castro Neto, *Phys. Rev. Lett.* **98**, 146801 (2007).
- [10] R. Nandkishore, L. S. Levitov, and A. V. Chubukov, *Nature Phys* **8**, 158 (2012).
- [11] Y. Cao, V. Fatemi, S. Fang, K. Watanabe, T. Taniguchi, E. Kaxiras, and P. Jarillo-Herrero, *Nature* **556**, 43 (2018).
- [12] H. Zhou, T. Xie, T. Taniguchi, K. Watanabe, and A. F. Young, *arXiv:2106.07640* (2021).
- [13] W. Kohn and J. M. Luttinger, *Phys. Rev. Lett.* **15**, 524 (1965).
- [14] Y. Takada, *J. Phys. Soc. Jpn.* **45**, 786 (1978).
- [15] H. Rietschel and L. J. Sham, *Phys. Rev. B* **28**, 5100 (1983).
- [16] J. Ruhman and P. A. Lee, *Phys. Rev. B* **94**, 224515 (2016).
- [17] P. Monthoux, D. Pines, and G. G. Lonzarich, *Nature* **450**, 1177 (2007).
- [18] M. A. Baranov, A. V. Chubukov, and M. Yu. Kagan, *Int. J. Mod. Phys. B* **06**, 2471 (1992).
- [19] A. V. Chubukov, *Phys. Rev. B* **48**, 1097 (1993).
- [20] V. M. Galitski and S. Das Sarma, *Phys. Rev. B* **67**, 144520 (2003).
- [21] V. Tolmachev and S. Tiablikov, *Sov. Phys. JETP* **7** (1958).
- [22] Y. Takada, *Phys. Rev. B* **39**, 11575 (1989).
- [23] Y. Takada, *Phys. Rev. B* **47**, 5202 (1993).
- [24] C. F. Richardson and N. W. Ashcroft, *Phys. Rev. B* **55**, 15130 (1997).
- [25] C. F. Richardson and N. W. Ashcroft, *Phys. Rev. Lett.* **78**, 118 (1997).
- [26] C. A. Kukkonen and A. W. Overhauser, *Phys. Rev. B* **20**, 550 (1979).
- [27] A. Chubukov, N. V. Prokof'ev, and B. V. Svistunov, *Phys. Rev. B* **100**, 064513 (2019).
- [28] J. Kaye, K. Chen, and O. Parcollet, *arxiv:2107.13094* (2021).
- [29] P. Morel and P. W. Anderson, *Phys. Rev.* **125**, 1263 (1962).

Supplemental materials

KUKKONEN-OVERHAUSER THEORY FOR THE HOMOGENEOUS COULOMB GAS

To properly resum the singular behavior at momentum transfer $q = 2k_F$ that ultimately leads to the Kohn-Luttinger mechanism, one needs to consider geometric series for the bubble and exchange diagrams on equal footing. Now, apart from the bare potential, the series

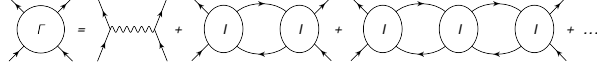


FIG. 1: Resummation of the particle-hole channel.

are built on the vertex I which contains all diagrams irreducible in the particle-hole channel.

Since the relevant part of all particle-hole irreducible diagrams has the same singularity, the assumption is that the relevant diagrams have the same functional form as in RPA. Thus, instead of computing the full particle-hole irreducible vertex I an approximation is used where I contains the bare potential and the G_{\pm} terms originating from exchange diagrams, while its functional form is that of an effective potential:

$$I \approx V - V(G_+ + G_- \vec{\sigma}_1 \cdot \vec{\sigma}_2). \quad (1)$$

This scheme accounts for all relevant singular contributions as long as the G_{\pm} functions are chosen appropriately.

Equation (1) leads to the standard expression for the KO vertex, and provides an opportunity to take full advantage of the well-studied ansatz for local field factors. In our simulations we employ the same ansatz as in Ref. [1, 2]. It is somewhat outdated for large values of r_s , but is more than adequate for $r_s \leq 2$ considered in our work when the difference between the KO and RPA treatments is very small.

DISCRETE LEHMANN REPRESENTATION FOR THE GAP-FUNCTION EQUATION

Since our goal is compact, accurate, and efficient processing of the frequency space, we omit momentum variables here for brevity. The eigenvalue problem to solve is given by Eq.(2) in the main text with the four-point vertex Γ approximated by $V_{KO}(\omega) = V + W(\omega)$, where V is the Coulomb potential and $W(\omega)$ is the frequency dependent part to be represented by the DLR. The gap-function Δ and the anomalous Green's function $F = GG\Delta$ are also assumed to be compatible with DLR for

asymmetric correlators:

$$W_m = \sum_{\alpha} W_{\alpha} K_c(m, \alpha), \quad (2)$$

$$F_n = \sum_{\alpha} F_{\alpha} K_a(n, \alpha), \quad (3)$$

$$\Delta_n = \sum_{\alpha} \Delta_{\alpha} K_a(n, \alpha), \quad (4)$$

with

$$K_c(m, \alpha) = \frac{2\alpha}{\alpha^2 + \omega_m^2} (1 - e^{-\alpha\beta}), \quad (5)$$

$$K_a(n, \alpha) = \frac{2\alpha}{\alpha^2 + \omega_n^2} (1 + e^{-\alpha\beta}). \quad (6)$$

Substituting these expressions in Eq.(2) in the main text we get

$$\begin{aligned} \lambda \Delta_n &= -T \sum_m [V + W_{n-m}] F_m \\ &= -TV \sum_{\alpha} F_{\alpha} \sum_m K_a(m, \alpha) \\ &\quad -T \sum_{\alpha, \gamma} W_{\gamma} F_{\alpha} \sum_m K_a(m, \alpha) K_c(n-m, \gamma). \end{aligned} \quad (7)$$

With pre-computed coefficients $S_{\alpha} = \sum_m K_a(m, \alpha)$ and $C_{n, \gamma, \alpha} = \sum_m K_a(m, \alpha) K_c(n-m, \gamma)$, the right hand side of the gap equation involves compact sums over α and γ . Moreover, simple analytical structure of K_c and K_a allows one to compute S_{α} and $C_{n, \gamma, \alpha}$ analytically:

$$\begin{aligned} S_{\alpha} &= \sum_m K_a(m, \alpha) \\ &= \sum_m \frac{2\alpha}{\alpha^2 + \omega_n^2} (1 + e^{-\alpha\beta}) \\ &= (1 + e^{-\alpha\beta}) \tanh(\alpha\beta/2) \end{aligned} \quad (8)$$

and

$$\begin{aligned} C_{n, \gamma, \alpha} &= \sum_m K_a(m, \alpha) K_c(n-m, \gamma) \\ &= \sum_m \frac{4\alpha\gamma(1 + e^{-\alpha\beta})(1 - e^{-\gamma\beta})}{(\alpha^2 + \omega_m^2)(\gamma^2 + (\omega_n - \omega_m)^2)} \\ &= \frac{4\alpha\gamma(1 + e^{-\alpha\beta})(1 - e^{-\gamma\beta})}{(\alpha^2 - \gamma^2)^2 + \omega_n^4 + 4\omega_n^2(\alpha^2 + \gamma^2)} \\ &\quad \left[\frac{\alpha^2 - \gamma^2 + \omega_n^2}{2\gamma} \frac{1 + e^{-\alpha\beta}}{1 - e^{-\alpha\beta}} \right. \\ &\quad \left. + \frac{\gamma^2 - \alpha^2 + \omega_n^2}{2\alpha} \frac{1 - e^{-\gamma\beta}}{1 + e^{-\gamma\beta}} \right] \end{aligned} \quad (9)$$

IMPLICIT RENORMALIZATION SCHEME AND ITS COMPATIBILITY WITH THE DISCRETE LEHMANN REPRESENTATION

In the IR approach the gap-function is split into the low- and high-energy parts using projection operators $P_m = \Theta(\Omega - |\omega_m|)$ and $\bar{P} = 1 - P$:

$$\Delta_n^{(L)} = P_n \Delta_n, \quad (10)$$

$$\Delta_n^{(H)} = \bar{P}_n \Delta_n. \quad (11)$$

The modified eigenvalue problem is formulated as

$$\bar{\lambda} \Delta_n^{(L)} = -P_n T \sum_m [V + W_{n-m}] F_m, \quad (12)$$

$$\Delta_n^{(H)} = -\bar{P}_n T \sum_m [V + W_{n-m}] F_m. \quad (13)$$

The problem is that sharp cutoffs in $\Delta^{(L)}$ and $\Delta^{(H)}$ cannot not be represented by the compact DLR. However, the right hand sides of these equations is compatible with DLR. Thus instead of $\Delta^{(L)}$ and $\Delta^{(H)}$ we store "complete versions" $\Delta^{(1)}$ and $\Delta^{(2)}$, and solve

$$\bar{\lambda} \Delta_n^{(1)} = -T \sum_m [V + W_{n-m}] F_m, \quad (14)$$

$$\Delta_n^{(2)} = -T \sum_m [V + W_{n-m}] F_m, \quad (15)$$

with $F = PF^{(1)} + (1-P)F^{(2)}$ calculated from the anomalous propagators based on $\Delta^{(1)}$ and $\Delta^{(2)}$. The main computational cost now looks as:

$$\begin{aligned} & -T \sum_m [V + W(\omega_n - \omega_m)] F(\omega_m) = \\ & -TV \sum_\alpha F_{1,\alpha} \sum_m P(\omega_m) K_a(m, \alpha) \\ & -TV \sum_\alpha F_{2,\alpha} \sum_m \bar{P}(\omega_m) K_a(m, \alpha) \\ & -T \sum_{\alpha, \gamma} W_\gamma F_{1,\alpha} \sum_m P(\omega_m) K_a(m, \alpha) K_c(n-m, \gamma) \\ & -T \sum_{\alpha, \gamma} W_\gamma F_{2,\alpha} \sum_m \bar{P}(\omega_m) K_a(m, \alpha) K_c(n-m, \gamma). \end{aligned} \quad (16)$$

Again, with predetermined coefficients describing sums over Matsubara frequencies we only need to handle compact sums. For the low-energy part these sums are done numerically; the high-energy part is obtained by subtracting the low-energy part from the analytic expressions (8) and (9).

[1] Y. Takada, Phys. Rev. B **39**, 11575 (1989).

[2] Y. Takada, Phys. Rev. B **47**, 5202 (1993)